



# Antibody-Based Immunotherapy To Treat and Prevent Infection with Hypervirulent *Klebsiella pneumoniae*

Elizabeth Diago-Navarro,<sup>a</sup> Isabel Calatayud-Baselga,<sup>b</sup> Donglei Sun,<sup>c</sup>  
Camille Khairallah,<sup>d</sup> Inderjit Mann,<sup>a</sup> Amaia Ulacia-Hernando,<sup>b</sup> Brian Sheridan,<sup>d</sup>  
Meiqing Shi,<sup>c</sup> Bettina C. Fries<sup>a,d</sup>

Department of Medicine (Division of Infectious Diseases), Stony Brook University, Stony Brook, New York, USA<sup>a</sup>; Universidad Francisco de Vitoria, Pozuelo de Alarcón, Madrid, Spain<sup>b</sup>; Department of Veterinary Medicine, University of Maryland at College Park, College Park, Maryland, USA<sup>c</sup>; Department of Molecular Genetics and Microbiology, Stony Brook University, Stony Brook, New York, USA<sup>d</sup>

**ABSTRACT** Hypervirulent *Klebsiella pneumoniae* (hvKp) strains are predicted to become a major threat in Asia if antibiotic resistance continues to spread. Anticapsular antibodies (Abs) were developed because disseminated infections caused by hvKp are associated with significant morbidity and mortality, even with antibiotic-sensitive strains. K1-serotype polysaccharide capsules (K1-CPS) are expressed by the majority of hvKp strains. In this study, K1-CPS-specific IgG Abs were generated by conjugation of K1-CPS to immunogenic anthrax protective antigen (PA) protein. Opsonophagocytic efficacy was measured *in vitro* and *in vivo* by intravital microscopy in murine livers. *In vivo* protection was tested in murine models, including a novel model for dissemination in hvKp-colonized mice. Protective efficacy of monoclonal antibodies (MAbs) 4C5 (IgG1) and 19A10 (IgG3) was demonstrated both in murine sepsis and pulmonary infection. In hvKp-colonized mice, MAb treatment significantly decreased dissemination of hvKp from the gut to mesenteric lymph nodes and organs. Intravital microscopy confirmed efficient opsonophagocytosis and clearance of bacteria from the liver. *In vitro* studies demonstrate that MAbs work predominantly by promoting FcR-mediated phagocytosis but also indicate that MAbs enhance the release of neutrophil extracellular traps (NETs). In anticipation of increasing antibiotic resistance, we propose further development of these and other *Klebsiella*-specific MAbs for therapeutic use.

**KEYWORDS** *Klebsiella pneumoniae*, hypervirulence, adjuvant therapy, monoclonal antibodies, colonization, opsonophagocytosis, intestinal colonization

**M**ultidrug-resistant *Klebsiella pneumoniae* strains have kept the medical community on high alert, as they have been spreading worldwide. The most successful clonal type in the United States is the ST258 clone (1), although other clones have been described as well (2). Less noticed but also concerning is the emergence of hypervirulent *K. pneumoniae* (hvKp) strains. These *K. pneumoniae* strains are phenotypically easily identified in the laboratory because they express a hypermucoid polysaccharide capsule, which traditional serotyping classified as a K1 serotype. These hvKp strains are much more virulent than the ST258 strain and kill mice in a few days (3). They cause community-acquired infections that rapidly progress to invasive disease in patients without major comorbidities (3). These strains have been reported worldwide (4, 5), but the majority of cases are in Asia, where hvKp is the leading cause of liver abscesses in Taiwan (6), Singapore (7), Hong Kong (8), and South Korea (9). In fact, in Taiwan, the annual incidence of pyogenic liver abscess has increased between 1996 and 2004 from 11 to 17 cases per 100,000 persons (10). A significant percentage of hvKp infections

Received 21 September 2016 Returned for modification 14 October 2016 Accepted 19 October 2016

Accepted manuscript posted online 26 October 2016

**Citation** Diago-Navarro E, Calatayud-Baselga I, Sun D, Khairallah C, Mann I, Ulacia-Hernando A, Sheridan B, Shi M, Fries BC. 2017. Antibody-based immunotherapy to treat and prevent infection with hypervirulent *Klebsiella pneumoniae*. *Clin Vaccine Immunol* 24:e00456-16. <https://doi.org/10.1128/CVI.00456-16>.

**Editor** Drusilla L. Burns, Food and Drug Administration

**Copyright** © 2017 American Society for Microbiology. All Rights Reserved.

Address correspondence to Bettina C. Fries, [bettina.fries@stonybrookmedicine.edu](mailto:bettina.fries@stonybrookmedicine.edu).

disseminate to the eye or meninges (11), commonly resulting in irreversible damage and mortality rates ranging from 3% to 42% (3). Epidemiological studies demonstrated that healthy adults carry virulent strains in their gastrointestinal tracts, and multilocus sequence typing (MLST) confirms a link between colonization and invasive infections in patients (12).

Fortunately and in contrast to ST258 strains (13), hvKp strains exhibit less diversity of their capsular polysaccharide (CPS). The K1 serotype is the prevailing CPS and is present in up to 81% of hvKp strains, followed by K2 and non-K1/K2 serotypes, respectively (3, 11). Most K1 serotype strains, but not all, are assigned to the ST23 clonal group by MLST (14). Until recently, hvKp strains were sensitive to standard antibiotics, so, if recognized early, infections caused by hvKp could be successfully treated despite their invasive nature. *In vitro* experiments demonstrated successful transfer of a KPC-bearing plasmid to an hvKp strain (15) and raised worries that *bla*<sub>KPC-2</sub> and *bla*<sub>KPC-3</sub> could emerge in an hvKp strain and cause infections in the community. In support of these concerns are reported rising antibiotic resistance in hvKp strains in China (16). Indeed, in 2014 and 2015 the first carbapenem-resistant hvKp strains were isolated from patients in China (17, 18).

Given the looming threat of emerging multidrug-resistant hvKp strains, we sought to develop novel therapeutic antibodies (Abs) targeting the CPS of these hvKp strains.

We present investigations with two monoclonal antibodies (MAbs) that promote phagocytosis by Kupffer cells in the liver and exhibit protective efficacy in three murine models, including one novel model that examines the effect of MAb treatment on dissemination in colonized mice.

## RESULTS

**Immunization with PA-conjugated K1-CPS.** Vaccination with K1-CPS conjugated to protective antigen (PA) enhanced immunogenicity and yielded 6 IgG-producing hybridomas (3 IgG1, 2 IgG3, and 1 IgG2a). The two selected hybridomas, 4C5 (IgG1) and 19A10 (IgG3), excreted high-affinity K1-CPS-specific MAbs. Coincubation with either MAb induced agglutination and quelling of 3 distinct K1 *K. pneumoniae* strains (Fig. 1A), whereas no agglutination was observed with 47 control non-K1 *K. pneumoniae* strains (13 and data not shown). Variable region (VR) sequence analysis established that the heavy chain (V<sub>H</sub>) of 19A10 is identical to that of the IGHV2-9\*02 family, whereas the V<sub>H</sub> of 4C5 is 95.79% identical (8 mutated residues) to the sequence of IGHV1S41\*01 family members (Table 1). The light chain (V<sub>L</sub>) of 19A10 is identical to that of IGKV1-117\*01, and that of 4C5 is 99.64% identical (1 base mutated) to the IGKV6-25\*01 germ line kappa sequence. Enzyme-linked immunosorbent assays (ELISAs) employing isotype-specific secondary Abs demonstrated simultaneous binding to purified CPS, consistent with nonoverlapping epitopes (data not shown).

**4C5 and 19A10 promote complement deposition and NETosis.** Although C3 complement (C3c) deposition on the capsule in the presence of binding of MAbs 4C5 and 19A10 was significantly increased by 44% and 17% compared to the phosphate-buffered saline (PBS) control (Fig. 1B) (*P* value of 0.0014 by analysis of variance [ANOVA], *P* value of <0.05 for PBS versus 4C5, nonsignificant *P* value for 19A10, *P* value of <0.001 for IgG control versus 4C5, and *P* value of <0.05 for 19A10), we observed deposition of the membrane attack complex (MAC) in K1 *K. pneumoniae* bacteria only after binding of 19A10 (Fig. 1C). Neutrophils can release web-like structures, called neutrophil extracellular traps (NETs), that trap and kill microbes (19). This process is called NETosis and can enhance the inflammatory response and clearance of microbes. We found K1 *K. pneumoniae* coincubated with either MAb 4C5 or 19A10 led to a significant release of NETs similar to NETs induced by hyphae of *Candida albicans* (20) (see Fig. S1 in the supplemental material). NETs were not induced by IgG control Ab or PBS (19).

**4C5 and 19A10 are opsonophagocytic Abs.** Promoting opsonophagocytic efficacy is considered a major predictor of antibody protective efficacy. Accordingly, MAb coincubation decreased K1 *K. pneumoniae* virulence in the *Galleria mellonella* model, which relies on phagocytic cells as its major host defense (*P* value by log-rank test of

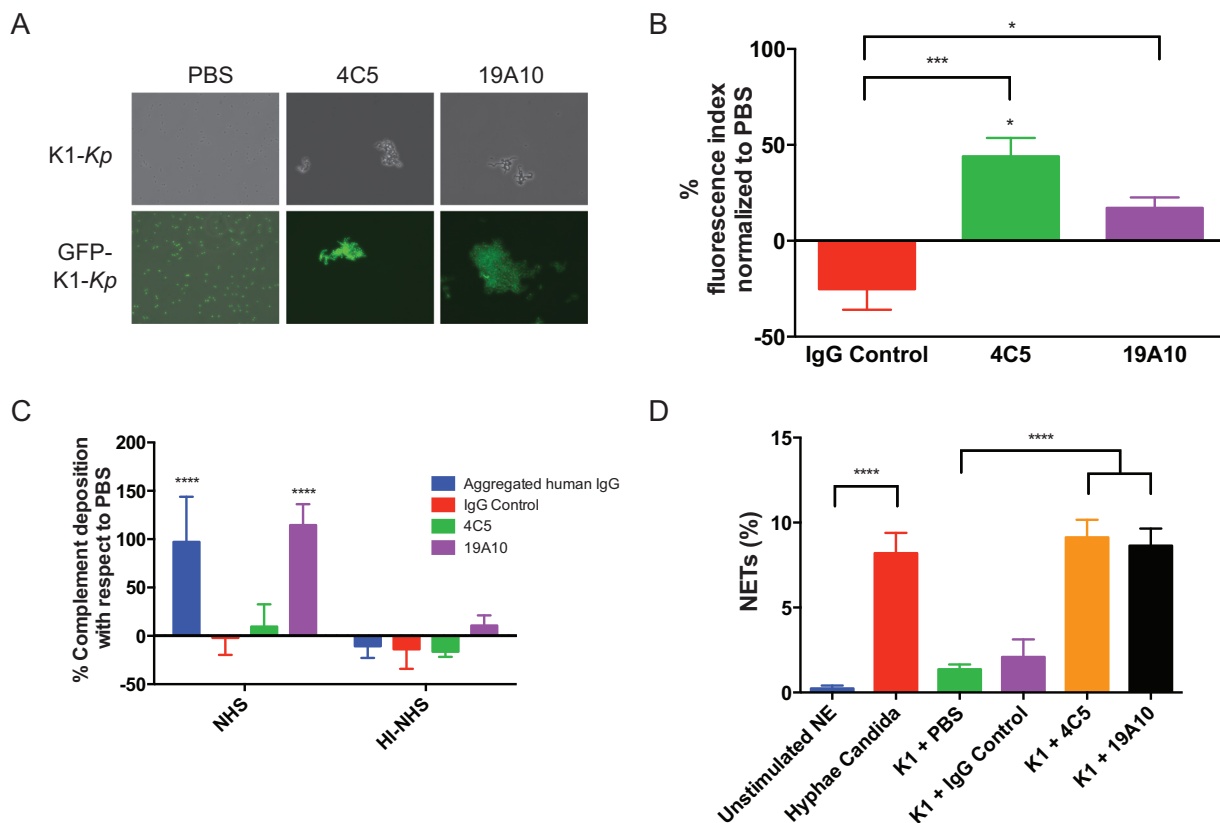


**FIG 1** (A) Agglutination of *K. pneumoniae* serotype K1 (K1-*Kp*) in the presence of 10  $\mu$ g of MAb. (Lower) Agglutination of the GFP-labeled *K. pneumoniae* strain. (B) Fluorescence signal of anti-human C3c fluorescein isothiocyanate (FITC) was measured in K1 *K. pneumoniae* bacteria incubated with MAbs and PBS. The mean percent increase of FITC signal relative to each PBS control is shown with standard deviations. (C) Binding of anti-human C5b-9 was measured by ELISA in K1-*K. pneumoniae* bacteria incubated with NHS or HI-NHS and MAbs, aggregated human IgG, or PBS. Mean percent increase of AP signal relative to each PBS control is shown with standard deviations from 3 replicates. *P* values were calculated by ANOVA with *post hoc* Tukey's multiple-comparison test. (D) Quantitation of NET release by human neutrophils after stimulation with *C. albicans*, K1 *K. pneumoniae*, or K1 *K. pneumoniae* incubated with MAbs 4C5 and 19A10 and an IgG control or unstimulated neutrophils (NE). Bars reflect mean percentages (with standard deviations) of neutrophil nuclei with an area exceeding 1,000  $\mu$ m<sup>2</sup> over the total neutrophils in the field (3 independent replicates). *P* values were determined by one-way ANOVA with Sidak's multiple-comparison test. \*, *P* < 0.05; \*\*\*, *P* < 0.001; \*\*\*\*, *P* < 0.0001.

0.0172 and 0.032 for 4C5 and 19A10, respectively) (Fig. S2). Accordingly, both 4C5 and 19A10 also promote uptake of K1 *K. pneumoniae* cells by primary murine macrophages. Specifically, opsonization with 4C5 and 19A10 significantly enhanced phagocytosis (22.5% and 42.4% for 4C5 and 14.9% and 25.5% for 19A10) (*P* value of <0.0022 by 2-way ANOVA and *P* values of <0.0022 and <0.0001 for PBS versus 4C5) (Fig. 2A and Movie S1b and c) at 67 and 105 min after infection. We evaluated if Fc-receptor engagement was required for phagocytosis. We found that phagocytosis was diminished in macrophages from Fc $\gamma$ R-deficient mice (Fig. 2A) (*P* value of 0.0001 by 2-way ANOVA, <0.0001 for both time points for 4C5, and 0.0022 and <0.0001 for 19A10 for each time point). Similar opsonophagocytic efficacy of the MAbs was confirmed with THP-1, a human monocyte cell line (Fig. 2B). Killing experiments performed in J744.16 cells demonstrated that killing occurred only in MAb-treated macrophages (Fig. S2B and C and Movie S1a) and not in control experiments.

**TABLE 1** Affinity and germ line VR gene usage of MAbs 4C5 and 19A10

MAb	<i>K<sub>d</sub></i> <sup>a</sup> (nM)	V <sub>H</sub> gene and family	J <sub>H</sub> gene	D gene	V <sub>L</sub> family	V <sub>L</sub> gene	J <sub>L</sub> gene
4C5	0.36 $\pm$ 0.072	X06868, IGHV1S41*01	IGHJ3*01	— <sup>b</sup>	IGKV6-25*01	AJ235962	IGKJ2*01
19A10	0.24 $\pm$ 0.032	AJ851868, IGHV2-9*02	IGHJ3*01	IGHD2-2*01	IGKV1-117*01	D00081	IGKJ1*01

<sup>a</sup>*K<sub>d</sub>*, dissociation constant.

<sup>b</sup>IMGT/junction analysis gives no results for this junction.

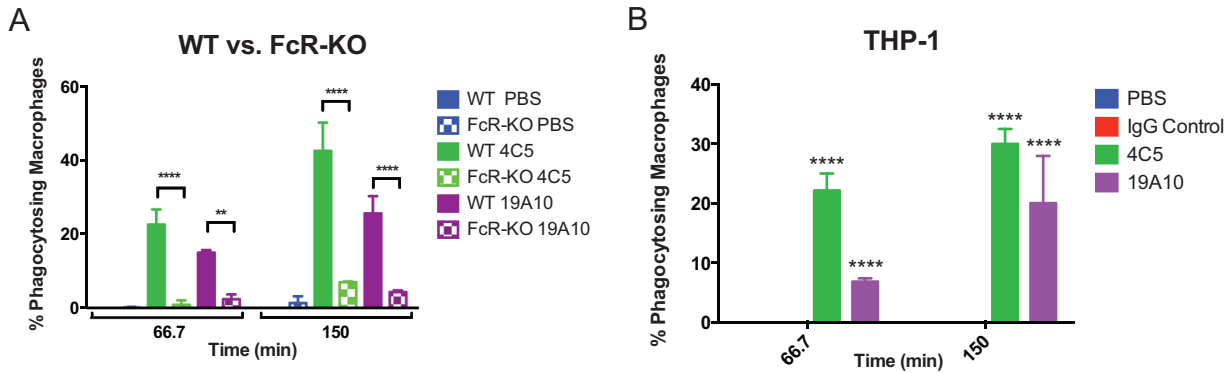


**FIG 2** (A) 4C5 and 19A10 enhance phagocytosis of K1 *K. pneumoniae* in bone marrow-derived wild-type macrophages but not in FcR-KO macrophages. (B) Opsonophagocytic efficacy was also seen in THP-1-differentiated human macrophages. Graphs depict mean percentages (with standard deviations) of macrophages with phagocytosed pH-rodo-labeled K1 *K. pneumoniae* after 67 and 105 min in three independent experiments. *P* values were determined by 2-way ANOVA with Tukey’s multiple-comparison test. \*\*, *P* < 0.01; \*\*\*\*, *P* < 0.0001.

**Treatment with 4C5 and 19A10 separately and in combination enhances survival of K1 *K. pneumoniae*-infected mice.** Protective efficacy next was investigated *in vivo* in two different murine infection models using K1 *K. pneumoniae* strain 20. For these experiments, Swiss-Webster mice were pretreated with PBS, 500 μg of an IgG isotype control, 4C5, 19A10, or a combination of both MABs (each at 250 μg). Treatment with 4C5 significantly enhanced survival compared to that for PBS- or sham-treated mice (*P* value of 0.0108) (Fig. 3A). MAb-treated mice also exhibited reduced bacterial burden (CFU) in liver, lung, and spleen compared to control-treated mice (*P* value of <0.0001 by ANOVA; *P* value for 4C5 of <0.0001) (Fig. 3B). For mice treated with 19A10, a similar protective trend (*P* = 0.068) and a significantly reduced bacterial organ burden (*P* value of <0.0001) were observed. Importantly, treatment with combinations of MABs (250 μg each) enhanced protective efficacy even further (*P* value of 0.0024)

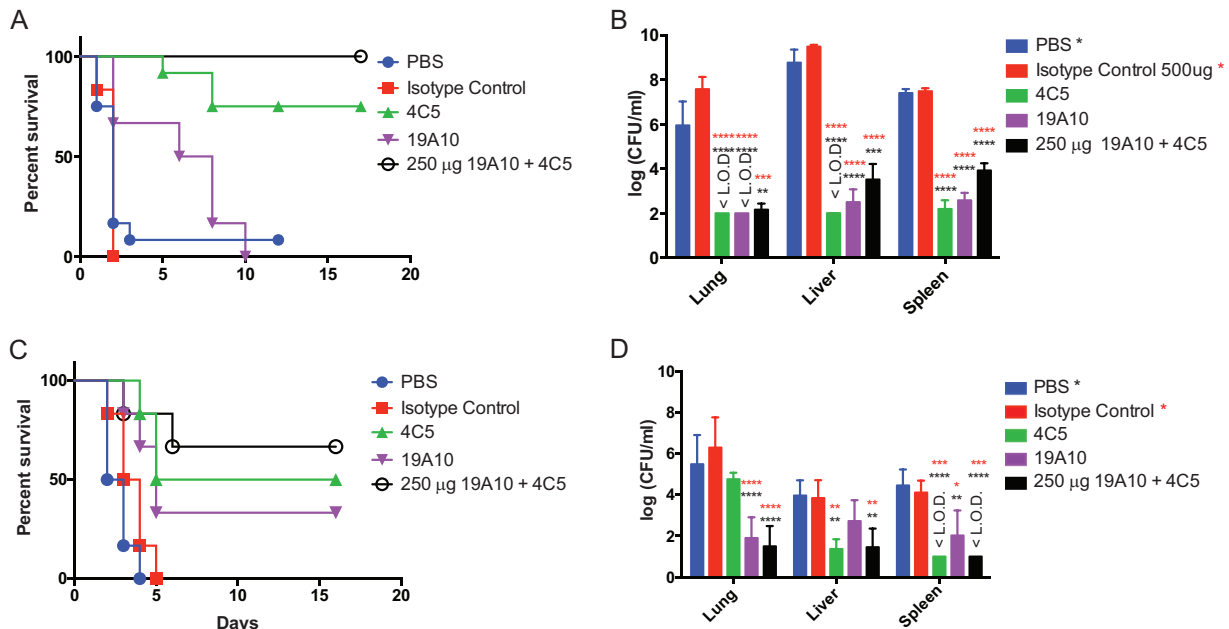


**FIG 3** (A) Survival analysis of mice (*n* = 6 per group) infected i.p. with 5 × 10<sup>4</sup> CFU of K1 *K. pneumoniae* and treated with PBS, 500 μg IgG control, 4C5, and 19A10, or 250 μg 4C5 and 19A10. (B and D) Shown are mean log CFU/ml (with standard deviations; *n* = 4 mice per group) at 24 h postinfection. Black asterisks denote comparisons of PBS and both MABs, and red asterisks denote comparisons with the IgG control. *P* values were determined by 2-way ANOVA with Tukey’s multiple-comparison test. (C) Survival analysis of mice (*n* = 6 per group) infected i.t. with 1 × 10<sup>4</sup> K1 *K. pneumoniae* and treated with PBS, 500 μg 4C5 and 19A10, or 250 μg 4C5 and 19A10. *P* values for panels A and C were determined with log-rank (Mantel-Cox) test corrected with Bonferroni’s multiple-comparison test. \*\*, *P* < 0.01; \*\*\*, *P* < 0.001; \*\*\*\*, *P* < 0.0001. <L.O.D. indicates the value is under the limit of detection.

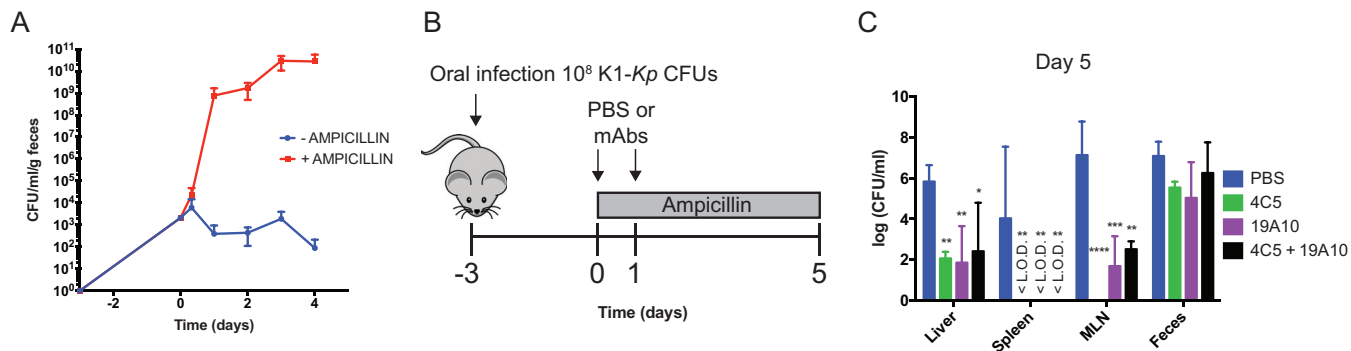


**FIG 4** (A) Bacterial CFU counts for feces of colonized mice increase more than 5 logs after ampicillin treatment. (B) Time of ampicillin and MAb treatment in colonized mice. (C) Mean bacterial loads in organs postdissemination and in feces on day 8 postcolonization with 10<sup>8</sup> CFU of K1 *K. pneumoniae*. Mean log CFU/ml with standard deviations (*n* = 3 mice per group) are shown. *P* values were determined by 2-way ANOVA with Dunnett’s multiple-comparison test. Asterisks denote comparisons to PBS. \*, *P* < 0.05; \*\*, *P* < 0.01; \*\*\*, *P* < 0.001; \*\*\*\*, *P* < 0.0001. <L.O.D indicates the value is under the limit of detection.

and also reduced bacterial burden significantly (*P* value of <0.0001). When MAb doses were lowered to 50% (250 μg, 12.5 mg/kg of body weight), similar protection was seen (Fig. S3A and B).

Similar trends were observed in an intratracheal infection (i.t.) model where mice were treated intravenously (i.v.) with PBS, isotype control, or MAbs alone or in combination 24 h before intratracheal inoculation of 10<sup>4</sup> CFU of K1 *K. pneumoniae*. Treatment with 4C5 exhibited superior protective efficacy in survival compared to 19A10 treatment (Fig. 3C) (*P* value for 4C5 treatment, 0.0048; *P* value for 19A10 treatment, 0.0244) and decreasing bacterial burden in organs (Fig. 3D) except in lungs. Survival (combination *P* value of 0.0116) as well as bacterial clearance were further enhanced in this model by treatment with MAb cocktail.

Cytokine levels of gamma interferon (IFN-γ), interleukin-1β (IL-1β), IL-2, IL-6, and tumor necrosis factor alpha (TNF-α) in liver and spleen homogenates of MAb-treated mice were significantly lower than those of sham-treated mice (*P* value of <0.0001 by 2-way ANOVA for both liver and spleen) (Fig. S3C and D). Similar trends were noted in lungs (Fig. S3E).

**Treatment with MAbs reduces ampicillin-induced dissemination from gut in K1 *K. pneumoniae*-colonized mice.** Protective efficacy of MAbs was examined in a murine model of gastrointestinal colonization, where bacterial dissemination to liver, spleen, and mesenteric lymph nodes (MLN) is promoted by treatment with antibiotics. Mice colonized with 10<sup>8</sup> CFU of green fluorescent protein (GFP)-labeled K1 *K. pneumoniae* via oral ingestion were given ampicillin, leading to a significant increase in bacterial burden in feces and subsequent translocation and dissemination to MLN, spleen, and liver (Fig. 4A to C). We investigated if MAb treatment protected against dissemination and decreased bacterial burden in MLN, spleen, and liver (Fig. 4B). Our data indicate that bacterial dissemination to the MLN, liver, and spleen was significantly decreased and bacterial burden was up to 6 logs lower in those organs compared to the PBS-treated mice (Fig. 4C) (*P* value of <0.0001 by 2-way ANOVA). In contrast, bacterial colonization seen in feces showed no significant differences with MAb treatment, indicating that colonization *per se* is not affected by systemic MAb treatment.

**Antibodies promote capture of K1 *K. pneumoniae* in the liver.** Kupffer cells in the liver are resident professional phagocytes and constitute a key component of the unique hepatic innate immune system, which is designed as a barrier between the digestive system and the rest of the body. Intravital microscopy (IVM) allows visualization of dynamic events in the hepatic microvasculature when mice are i.v. injected with 10<sup>8</sup> CFU of GFP-labeled kvKp. Time-lapse video demonstrated significantly higher numbers of captured bacteria and decreased presence of bacteria flowing through blood vessels when mice were treated with K1-specific MAbs (*P* value of <0.0001 by ANOVA; MAb treatment had different *P* values of <0.05 at different time points) (Fig. 5A and B; Video



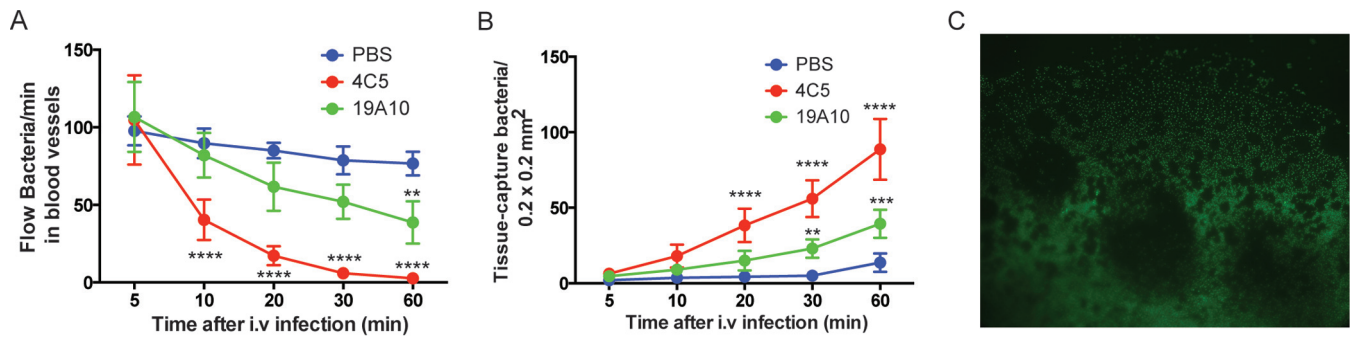


**FIG 5** (A) Number of bacteria passing a fixed point in the sinusoid blood vessel at various time points after injection in intravital microscopy. (B) The number of stationary bacteria captured in a field of view at various time points after injection. For each group ( $n = 3$  mice) in panels A and B, mice were left untreated or were treated with MAb and i.v. injection of  $1 \times 10^8$  GFP-expressing K1 *K. pneumoniae* CFU. A 1-h IVM video was taken based on the protocol described in the text. Means with standard deviations at different times are shown. *P* values were determined by 2-way ANOVA with Tukey's multiple-comparison test. \*\*,  $P < 0.01$ ; \*\*\*,  $P < 0.001$ ; \*\*\*\*,  $P < 0.0001$ . (C) Microscopy image (200 $\times$ ) of the intraabdominal cavity of untreated mouse after i.p. injection of  $5 \times 10^4$  CFU of GFP-expressing K1 *K. pneumoniae*.

S2a and b) compared to control-treated mice (Video S2c). When lower numbers of bacteria ( $5 \times 10^4$  CFU) were injected intraperitoneally (i.p.) with K1-specific MAbs, K1 *K. pneumoniae* bacteria were completely cleared. No bacteria were detected in the blood vessels or captured in the tissue ( $P < 0.001$  and  $P = 0.0014$ , respectively, by ANOVA) (Fig. S4A and B, Video S3a and b). Without concomitant MAb treatment, K1 *K. pneumoniae* bacteria were detected abundantly in the abdominal cavity (Fig. 5C; Fig. S4C and Video S3c). In summary, these findings demonstrate that MAb treatment enables the liver to be an effective barrier because of efficient opsonophagocytic action promoted by K1-specific MAb treatment.

## DISCUSSION

Polysaccharide capsules of diverse microbes elicit protective immune responses in the host (21, 22). Clinical data from patients with recurrent hvKp-mediated liver abscesses indicate that opsonizing and killing efficacy of serum increases over time, consistent with an evolving protective antibody response (23). We now present two lead MAbs that control invasive infections caused by an hvKp strain.

Common protective characteristics were observed with both MAbs, although they differ in isotype and bind distinct nonoverlapping epitopes. The capsule of hvKp strains evades the human immune response by inhibiting binding of complement, which can kill on its own or promote phagocytosis (24). Only IgG3 MAb 19A10 elicited enhanced terminal complex (MAC) formation, although both MAbs promoted C3c deposition. Isotype-specific differences in complement activation and protective efficacy have been described (25, 26). Also, others have shown that IgG1 MAbs can be highly protective anti-CPS MAbs and exhibit superior Fc $\gamma$ R activation signaling compared to IgG3 Abs (27), which could explain higher efficacy even in the context of comparable binding affinities. Ultimately, experiments with isotype switch variants are warranted to optimize isotype choice prior to MAb humanization.

Ab-opsonized K1 *K. pneumoniae* is predominantly Fc $\gamma$ R mediated. Ab-opsonized *Salmonella* escapes from the phagolysosome (28); under our experimental conditions we cannot determine if MAbs promote phagolysosomal escape, as they are already killed. Protection was demonstrated in two murine infection models, and consistent with our *in vitro* data, we found 4C5 was superior to 19A10. Although we found an incremental increase of the bacterial burden with the use of combination therapy compared to the use of each MAb alone, our data also show that combining MAbs, which mimics a protective polyclonal host immune response, can enhance that passive immunotherapy.

Protective efficacy of MAbs in a colonization model supports a novel indication for antimicrobial MAbs. *Klebsiella* infections in the liver originate from the gut, which is colonized with the bacteria in a significant percentage of Asian patients (29). It has been

shown that in colonized mice ampicillin use increases the risk of hvKp-induced liver abscess (30). Thus, it is reasonable to expect similar risks in humans who are treated with antibiotics that cause major qualitative changes in the gut microbiome. We demonstrate in the event of dissemination from the gut that the number of bacterial CFU in MLN, spleen, and liver was significantly decreased when mice were pretreated with CPS-specific MAbs. This finding also has potential implications for preventing infections in patients colonized with carbapenem-resistant *K. pneumoniae* strains (ST258 clone), which result in disease in 50% of cases (31, 32). Based on our data, we propose that these patients could receive prophylactic MAb therapy that is specific for the capsules of those strains prior to receiving broad-spectrum antibiotics to prevent dissemination and disease.

Intravital microscopy investigates in real time the host-pathogen interaction in liver sinusoids (3), which are lined by phagocytic Kupffer cells that create a highly efficient filtering system. Altered cytokine expression in tissue of treated cells may be the result of MAb-modulated phagocyte-K1 *K. pneumoniae* interaction, which could further alter recruitment of neutrophils as described in other infections (33). During overwhelming infection or in the microenvironment of an abscess, phagocytosis alone may not be sufficient to clear an infection. Murine infection models show that mice with impaired capacity to form NETs are more prone to *K. pneumoniae* infections, indicating that NETs are relevant for successful clearance (34). Our observation that K1-specific MAbs promote NETosis is therefore consistent with these data and suggests additional mechanisms for MAb-based protection are operative. We propose that specific MAb agglutinates *K. pneumoniae*, cross-links Fc receptors, and promotes NET release.

Compared to triumphs seen with antitumor and anti-inflammatory MAb treatment, progress with anti-infective MAb development regrettably lags behind. This is surprising given the protective efficacy of hyperimmune-globulin preparations (35) and the overwhelming evidence with anti-infective Abs. They can work (36) as monotherapy, cocktails, or in combination with antimicrobial drugs (37). One problem may be that MAb cocktails commonly are more efficacious than monotherapy, especially if rapidly expanding pathogen populations are to be contained. With revised FDA licensing rules for MAbs, it has become easier to receive FDA approval for cocktails. Accordingly, MAb cocktails for treatment of *Clostridium difficile*, rabies prophylaxis (38, 39), and Ebola virus (40) are now being tested in advanced clinical trials. Another obstacle is strain variability, which is inherently underestimated by research with laboratory-adapted strains. This is also an especially major challenge for *K. pneumoniae* strains of the ST258 clonal background, as their CPS is very heterogenous. Both cross-reactive MAbs (13) as well as MAbs recognizing more universal targets can be developed to overcome this barrier. Recent work with MAbs to the polysaccharide poly-( $\beta$ -1,6)-*N*-acetylglucosamine are encouraging (41), and future studies should be done comparing efficacy of MAbs with differences in degree of microbial specificity. The spread of multidrug-resistant (MDR) bacteria in the community as exemplified now by MDR hvKp is a crucial development, associated not only with increased morbidity, mortality, and health care costs but also with inappropriate antibiotic use (42). Our findings may have broader implications, because treatment with anti-infective MAbs against a gut-colonizing bacteria like hvKp is a targeted intervention that should not disturb the microbiome, promote resistance, or lead to emergence of other serotypes. Our data support efforts to develop anti-infective antibodies, which, as evidenced by the efficacy of palivizumab, a MAb-based therapy against respiratory syncytial virus (RSV), in preterm infants, will even be effective in immunocompromised hosts. With continuous fast-moving globalization and unrestrained antibiotic usage, MDR bacteria are likely to become an increasing problem.

## MATERIALS AND METHODS

**K1 *K. pneumoniae* strains.** K1 *K. pneumoniae* strains ( $n = 4$ ) were collected from patients at Montefiore Medical Center (MMC) and Stony Brook University (SBU) Hospital. One strain was kindly provided by Thomas Russo at the University at Buffalo, SUNY. *K. pneumoniae* strains were cultured in Luria-Bertani (LB) broth or agar plates at 37°C. *K. pneumoniae* strain 20, of clonal sequence type ST23 that

expresses K1-CPS, was used for CPS purification and for *in vitro* and *in vivo* experiments (13). The strain was GFP labeled with pPROBEKT plasmid kindly provided by E. W. Triplett (43).

**CPS purification and conjugation.** K1-CPS was isolated for conjugation with protective antigen (PA) from *Bacillus anthracis* (see Methods S1 in the supplemental material). For conjugation, K1-CPS was activated with 1-cyano-4-dimethylaminopyridinium tetrafluoroborate (CDAP) as described previously, with modifications (13, 44) (Methods S1).

**MAb generation and characterization.** MAbs to K1-CPS were generated by immunization of BALB/c mice with 100  $\mu$ g of PA-conjugated K1-CPS in complete Freund's adjuvant followed by boosters of PA-conjugated K1-CPS in incomplete Freund's adjuvant. Fusion and cloning were performed as described previously (45). GenScript sequenced the variable region (VR) of 19A10- and 4C5-generated MAbs, which were analyzed using International ImMunoGeneTics (IMGT) Information System software. MAb affinity was determined by enzyme-linked immunosorbent assay (ELISA); briefly, decreasing concentrations of the MAbs were incubated for 1 h at 37°C onto a 0.5  $\mu$ g/ml K1-CPS-coated plate, and the binding was detected with the appropriate alkaline phosphatase (AP)-labeled secondary MAb.

**Agglutination assays.** Agglutination was carried out on glass slides as described previously (21). Briefly, 100  $\mu$ l of PBS with  $3 \times 10^6$  CFU of K1 *K. pneumoniae* was incubated with or without the MAbs (20  $\mu$ g) for 1 h at room temperature. Agglutination was observed under the microscope at  $\times 200$ .

**C3 and MAC complement deposition assays.** Deposition of C3c was measured by flow cytometry as described previously (46) (Methods S1). For MAC deposition assays, an overnight culture of serotype K1 was resuspended ( $2 \times 10^5$  CFU of K1) in 100  $\mu$ l of normal human serum (NHS) or heat-inactivated NHS (HI-NHS) (56°C for 1 h). Ten micrograms of either aggregated human IgG (classical positive control for classical pathway), IgG control, 4C5, or 19A10 then was added, incubated for 1 h at 37°C, and washed  $2 \times$  with buffer. Pellets were resuspended with biotin-labeled anti-human C5b-9 (Quidel) (1:500 dilution) and incubated for 1 h at 37°C. After repeated washing, streptavidin-AP (Vectastain ABC-AP) was added and incubated for 30 min at room temperature. After washing, pellets were resuspended in AP-substrate buffer and the  $A_{405}$  was measured. Results are expressed by the increment of the AP signal of MAb treatment with respect to PBS incubation.

**Galleria mellonella virulence assays.** Virulence of K1 *K. pneumoniae* was assessed in *G. mellonella* as previously reported (13) (Methods S1).

**Phagocytosis experiments.** The J744.16 murine macrophage cell line, THP-1 human monocyte cell line, and murine primary bone marrow macrophages were used for phagocytosis assays with bacteria labeled by pHrodo (Life Technologies). THP-1 cells (and J744.16 cells), differentiated with phorbol 12-myristate 12-acetate (PMA), were seeded at a concentration of  $5 \times 10^5$  in 35-mm glass-bottom microwell dishes (MatTek Corporation) and incubated with pHrodo-labeled K1 *K. pneumoniae* cells for 1 h with PBS and with 20  $\mu$ g of isotype control, 4C5, or 19A10 MAb at a multiplicity of infection of 10:1. Phagocytosis was immediately assessed using a Zeiss Axiovert 200M inverted microscope with a  $10 \times$  objective with the dish housed in an enclosed chamber under conditions of 5% CO<sub>2</sub> and 37°C. Images were taken every 3 min for the 2-h duration of the experiment. Phagocytosis was measured by counting the percentage of macrophages that display labeled bacteria at 67 and 105 min. Primary bone marrow macrophages were isolated as described previously (47) from wild-type or FcR knockout (KO) mice (*Fc $\gamma$ R1<sup>tm1Rav</sup>*; The Jackson Laboratory). After 7 days of macrophage differentiation, phagocytosis experiments were carried out as outlined above. Three independent experiments were performed. *In vitro* killing of K1 *K. pneumoniae* was investigated in the J744.16 macrophage cell line as previously reported (48) (Methods S1).

**NETosis experiments.** NETosis assays were carried out with human neutrophils as described previously (20), with modifications (Methods S1).

**In vivo mouse experiments.** Six- to 8-week-old female Swiss Webster mice (Taconic Biosciences) ( $n = 10$ ) were injected intraperitoneally (i.p.) with PBS, with 500  $\mu$ g or 250  $\mu$ g of control isotype, 4C5, and 19A10, or with 250  $\mu$ g or 125  $\mu$ g of 4C5 and 19A10 MAbs 120 min prior to challenge with  $5 \times 10^4$  CFU of K1 *K. pneumoniae* i.p. (sepsis model) or were treated i.p. 24 h prior to intratracheal (i.t.) challenge with  $10^4$  CFU of K1 *K. pneumoniae* (pulmonary infection model). Survival of 6 mice was monitored for 15 days. Liver, spleen, and lungs of 4 mice were processed to enumerate bacteria in homogenized tissue. Cytokine levels in homogenized tissue were analyzed using the ProcartaPlex mouse Th1/Th2 cytokine panel (Affymetrix) according to the manufacturer's recommendations. Gastrointestinal colonization was performed as described previously, with modifications for *K. pneumoniae* (49). Briefly, mice were deprived of food and water for 4 h prior to infection. Individually housed mice then were given a 0.5-cm<sup>3</sup> piece of bread inoculated with  $1 \times 10^8$  CFU of GFP-labeled K1 *K. pneumoniae* in PBS. On day 3 postinfection, mice were provided with water supplemented with 0.5 g/liter of ampicillin for the duration of the experiment. In addition, on days 3 and 4 mice received a dose of PBS, 500  $\mu$ g of 4C5 and 19A10, or 250  $\mu$ g of 4C5 and 19A10 i.v. On day 8, mice were euthanized and organs and tissues were prepared as previously described (49).

**IVM.** A liver intravital protocol was carried out as previously described (50) (Methods S1).

**Statistical analysis.** Statistical tests were performed with GraphPad Prism 6 for Mac. For multigroup comparisons of parametric data (e.g., phagocytosis, log-transformed CFU, and complement deposition), ANOVA with *post hoc* analysis using Tukey's, Sidak's, or Dunnett's comparison test was used. For two-group comparisons of parametric data (log-transformed CFU), paired *t* tests corrected for multiple comparisons using the Holm-Sidak method were performed. Survival analysis was performed using a log-rank (Mantel-Cox) test corrected with Bonferroni's multiple-comparison test.

**Ethics statement.** Animal study protocols were approved by the Animal Committee (IACUC) at Stony Brook University, approval number 628253, and by the Animal Committee (IACUC) at the University of



Maryland, approval number 340281. The study was performed in strict accordance with federal, state, local, and institutional guidelines that include the *Guide for the Care and Use of Laboratory Animals* (51), the Animal Welfare Act, and the *Public Health Service Policy on Humane Care and Use of Laboratory Animals* (52). All surgery was performed under ketamine and xylazine anesthesia, and every effort was made to minimize suffering. Human studies were approved by the Stony Brook University Human Subjects Committee (IRB), approval number 718744. Healthy donors gave written informed consent for blood extraction.

## SUPPLEMENTAL MATERIAL

Supplemental material for this article may be found at <https://doi.org/10.1128/CVI.00456-16>.

**TEXT S1**, PDF file, 0.08 MB

**TEXT S2**, PDF file, 0.3 MB.

**TEXT S3**, PDF file, 0.03 MB.

**VIDEO S1**, MOV file, 6.5 MB.

**VIDEO S2**, MOV file, 2.7 MB.

**VIDEO S3**, MOV file, 2.3 MB.

## ACKNOWLEDGMENTS

We thank Berhane Ghebrehiwet for technical help with the complement deposition assays.

B.C.F. was supported by NIH grant R21 AI114259. M.S. was supported by University of Maryland, Maryland Agricultural Experiment Station Competitive Grant Program for FY 2013 and FY 2016-2017 and NIH AI115086A. E.D.-N. was supported by Stony Brook University Medicine Pilot Grant 2016.

The funders had no role in study design, data collection and interpretation, or the decision to submit the work for publication.

## REFERENCES

- Chen L, Mathema B, Pitout JD, DeLeo FR, Kreiswirth BN. 2014. Epidemic *Klebsiella pneumoniae* ST258 is a hybrid strain. *mBio* 5:e01355-14. <https://doi.org/10.1128/mBio.01355-14>.
- Ocampo AM, Chen L, Cienfuegos AV, Roncancio G, Chavda KD, Kreiswirth BN, Jimenez JN. 2016. A two-year surveillance in five Colombian tertiary care hospitals reveals high frequency of non-cg258 clones of carbapenem-resistant *Klebsiella pneumoniae* with distinct clinical characteristics. *Antimicrob Agents Chemother* 60:332–342. <https://doi.org/10.1128/AAC.01775-15>.
- Shon AS, Bajwa RP, Russo TA. 2013. Hypervirulent (hypermucoviscous) *Klebsiella pneumoniae*: a new and dangerous breed. *Virulence* 4:107–118. <https://doi.org/10.4161/viru.22718>.
- Vila A, Cassata A, Pagella H, Amadio C, Yeh KM, Chang FY, Siu LK. 2011. Appearance of *Klebsiella pneumoniae* liver abscess syndrome in Argentina: case report and review of molecular mechanisms of pathogenesis. *Open Microbiol J* 5:107–113. <https://doi.org/10.2174/1874285801105010107>.
- Turton JF, Englender H, Gabriel SN, Turton SE, Kaufmann ME, Pitt TL. 2007. Genetically similar isolates of *Klebsiella pneumoniae* serotype K1 causing liver abscesses in three continents. *J Med Microbiol* 56:593–597. <https://doi.org/10.1099/jmm.0.46964-0>.
- Chang FY, Chou MY. 1995. Comparison of pyogenic liver abscesses caused by *Klebsiella pneumoniae* and non-*K. pneumoniae* pathogens. *J Formos Med Assoc* 94:232–237.
- Yeoh KG, Yap I, Wong ST, Wee A, Guan R, Kang JY. 1997. Tropical liver abscess. *Postgrad Med J* 73:89–92. <https://doi.org/10.1136/pgmj.73.856.89>.
- Lok KH, Li KF, Li KK, Szeto ML. 2008. Pyogenic liver abscess: clinical profile, microbiological characteristics, and management in a Hong Kong hospital. *J Microbiol Immunol Infect* 41:483–490.
- Chung DR, Lee SS, Lee HR, Kim HB, Choi HJ, Eom JS, Kim JS, Choi YH, Lee JS, Chung MH, Kim YS, Lee H, Lee MS, Park CK, Korean Study Group for Liver Abscess. 2007. Emerging invasive liver abscess caused by K1 serotype *Klebsiella pneumoniae* in Korea. *J Infect* 54:578–583. <https://doi.org/10.1016/j.jinf.2006.11.008>.
- Tsai FC, Huang YT, Chang LY, Wang JT. 2008. Pyogenic liver abscess as endemic disease, Taiwan. *Emerg Infect Dis* 14:1592–1600. <https://doi.org/10.3201/eid1410.071254>.
- Fang CT, Lai SY, Yi WC, Hsueh PR, Liu KL, Chang SC. 2007. *Klebsiella pneumoniae* genotype K1: an emerging pathogen that causes septic ocular or central nervous system complications from pyogenic liver abscess. *Clin Infect Dis* 45:284–293. <https://doi.org/10.1086/519262>.
- Lin JC, Koh TH, Lee N, Fung CP, Chang FY, Tsai YK, Ip M, Siu LK. 2014. Genotypes and virulence in serotype K2 *Klebsiella pneumoniae* from liver abscess and non-infectious carriers in Hong Kong, Singapore and Taiwan. *Gut Pathog* 6:21. <https://doi.org/10.1186/1757-4749-6-21>.
- Diago-Navarro E, Chen L, Passet V, Burack S, Ulacia-Hernando A, Kodiyankal RP, Levi MH, Brisse S, Kreiswirth BN, Fries BC. 2014. Carbapenem-resistant *Klebsiella pneumoniae* exhibit variability in capsular polysaccharide and capsule associated virulence traits. *J Infect Dis* 210:803–813. <https://doi.org/10.1093/infdis/jiu157>.
- Siu LK, Fung CP, Chang FY, Lee N, Yeh KM, Koh TH, Ip M. 2011. Molecular typing and virulence analysis of serotype K1 *Klebsiella pneumoniae* strains isolated from liver abscess patients and stool samples from noninfectious subjects in Hong Kong, Singapore, and Taiwan. *J Clin Microbiol* 49:3761–3765. <https://doi.org/10.1128/JCM.00977-11>.
- Siu LK, Huang DB, Chiang T. 2014. Plasmid transferability of *KPC* into a virulent K2 serotype *Klebsiella pneumoniae*. *BMC Infect Dis* 14:176. <https://doi.org/10.1186/1471-2334-14-176>.
- Li W, Sun G, Yu Y, Li N, Chen M, Jin R, Jiao Y, Wu H. 2014. Increasing occurrence of antimicrobial-resistant hypervirulent (hypermucoviscous) *Klebsiella pneumoniae* isolates in China. *Clin Infect Dis* 58:225–232. <https://doi.org/10.1093/cid/cit675>.
- Zhang R, Wang X, Lu J. 2014. Isolation of a carbapenem-resistant K1 serotype *Klebsiella pneumoniae* strain and the study of resistance mechanism. *Zhonghua Yi Xue Za Zhi* 94:3666–3670.
- Yao B, Xiao X, Wang F, Zhou L, Zhang X, Zhang J. 2015. Clinical and molecular characteristics of multi-clone carbapenem-resistant hypervirulent (hypermucoviscous) *Klebsiella pneumoniae* isolates in a tertiary hospital in Beijing, China. *Int J Infect Dis* 37:107–112. <https://doi.org/10.1016/j.ijid.2015.06.023>.
- Branzk N, Papayannopoulos V. 2013. Molecular mechanisms regulating

- NETosis in infection and disease. *Semin Immunopathol* 35:513–530. <https://doi.org/10.1007/s00281-013-0384-6>.
20. Branzk N, Lubojemska A, Hardison SE, Wang Q, Gutierrez MG, Brown GD, Papayannopoulos V. 2014. Neutrophils sense microbe size and selectively release neutrophil extracellular traps in response to large pathogens. *Nat Immunol* 15:1017–1025. <https://doi.org/10.1038/ni.2987>.
  21. Wu MF, Yang CY, Lin TL, Wang JT, Yang FL, Wu SH, Hu BS, Chou TY, Tsai MD, Lin CH, Hsieh SL. 2009. Humoral immunity against capsule polysaccharide protects the host from magA+ *Klebsiella pneumoniae*-induced lethal disease by evading Toll-like receptor 4 signaling. *Infect Immun* 77:615–621. <https://doi.org/10.1128/IAI.00931-08>.
  22. Chen T, Blanc C, Eder AZ, Prados-Rosales R, Souza AC, Kim RS, Glatman-Freedman A, Joe M, Bai Y, Lowary TL, Tanner R, Brennan MJ, Fletcher HA, McShane H, Casadevall A, Achkar JM. 2016. Association of human antibodies to arabinomannan with enhanced mycobacterial opsonophagocytosis and intracellular growth reduction. *J Infect Dis* 214:300–310. <https://doi.org/10.1093/infdis/jiw141>.
  23. Yeh FC, Yeh KM, Siu LK, Fung CP, Yang YS, Lin JC, Chang FY. 2012. Increasing opsonizing and killing effect of serum from patients with recurrent K1 *Klebsiella pneumoniae* liver abscess. *J Microbiol Immunol Infect* 45:141–146. <https://doi.org/10.1016/j.jmii.2011.12.006>.
  24. Tomas JM, Campubri S, Williams P. 1988. Surface exposure of the O-antigen in *Klebsiella pneumoniae* O1:K1 serotype strains. *Microb Pathog* 5:141–147. [https://doi.org/10.1016/0882-4010\(88\)90016-2](https://doi.org/10.1016/0882-4010(88)90016-2).
  25. Hovenden M, Hubbard MA, Aucoin DP, Thorkildson P, Reed DE, Welch WH, Lyons CR, Lovchik JA, Kozel TR. 2013. IgG subclass and heavy chain domains contribute to binding and protection by mAbs to the poly gamma-D-glutamic acid capsular antigen of *Bacillus anthracis*. *PLoS Pathog* 9:e1003306. <https://doi.org/10.1371/journal.ppat.1003306>.
  26. Sensel MG, Kane LM, Morrison SL. 1997. Amino acid differences in the N-terminus of C(H)2 influence the relative abilities of IgG2 and IgG3 to activate complement. *Mol Immunol* 34:1019–1029. [https://doi.org/10.1016/S0161-5890\(97\)00112-0](https://doi.org/10.1016/S0161-5890(97)00112-0).
  27. Nimmerjahn F, Ravetch JV. 2005. Divergent immunoglobulin G subclass activity through selective Fc receptor binding. *Science* 310:1510–1512. <https://doi.org/10.1126/science.1118948>.
  28. Vidarsson G, Stemerding AM, Stapleton NM, Spliethoff SE, Janssen H, Rebers FE, de Haas M, van de Winkel JG. 2006. FcRn: an IgG receptor on phagocytes with a novel role in phagocytosis. *Blood* 108:3573–3579. <https://doi.org/10.1182/blood-2006-05-024539>.
  29. Lin YT, Siu LK, Lin JC, Chen TL, Tseng CP, Yeh KM, Chang FY, Fung CP. 2012. Seroepidemiology of *Klebsiella pneumoniae* colonizing the intestinal tract of healthy Chinese and overseas Chinese adults in Asian countries. *BMC Microbiol* 12:13. <https://doi.org/10.1186/1471-2180-12-13>.
  30. Lin YT, Liu CJ, Yeh YC, Chen TJ, Fung CP. 2013. Ampicillin and amoxicillin use and the risk of *Klebsiella pneumoniae* liver abscess in Taiwan. *J Infect Dis* 208:211–217. <https://doi.org/10.1093/infdis/jit157>.
  31. Calfee D, Jenkins SG. 2008. Use of active surveillance cultures to detect asymptomatic colonization with carbapenem-resistant *Klebsiella pneumoniae* in intensive care unit patients. *Infect Control Hosp Epidemiol* 29:966–968. <https://doi.org/10.1086/590661>.
  32. Giannella M, Trecarichi EM, De Rosa FG, Del Bono V, Bassetti M, Lewis RE, Losito AR, Corcione S, Saffiotti C, Bartoletti M, Maiuro G, Cardellino CS, Tedeschi S, Cauda R, Viscoli C, Viale P, Tumbarello M. 2014. Risk factors for carbapenem-resistant *Klebsiella pneumoniae* bloodstream infection among rectal carriers: a prospective observational multicentre study. *Clin Microbiol Infect* 20:1357–1362. <https://doi.org/10.1111/1469-0691.12747>.
  33. Marques PE, Oliveira AG, Chang L, Paula-Neto HA, Menezes GB. 2015. Understanding liver immunology using intravital microscopy. *J Hepatol* 63:733–742. <https://doi.org/10.1016/j.jhep.2015.05.027>.
  34. Papayannopoulos V, Metzler KD, Hakkim A, Zychlinsky A. 2010. Neutrophil elastase and myeloperoxidase regulate the formation of neutrophil extracellular traps. *J Cell Biol* 191:677–691. <https://doi.org/10.1083/jcb.201006052>.
  35. Rossmann FS, Kropec A, Laverde D, Saaverda FR, Wobser D, Huebner J. 2015. In vitro and in vivo activity of hyperimmune globulin preparations against multiresistant nosocomial pathogens. *Infection* 43:169–175. <https://doi.org/10.1007/s15010-014-0706-1>.
  36. Saylor C, Dadachova E, Casadevall A. 2009. Monoclonal antibody-based therapies for microbial diseases. *Vaccine* 27(Suppl 6):G38–G46. <https://doi.org/10.1016/j.vaccine.2009.09.105>.
  37. Varshney AK, Wang X, MacIntyre J, Zollner RS, Kelleher K, Kovalenko OV, Pechuan X, Byrne FR, Fries BC. 2014. Humanized staphylococcal enterotoxin B (SEB)-specific monoclonal antibodies protect from SEB intoxication and *Staphylococcus aureus* infections alone or as adjunctive therapy with vancomycin. *J Infect Dis* 210:973–981. <https://doi.org/10.1093/infdis/jiu198>.
  38. Bakker AB, Python C, Kissling CJ, Pandya P, Marissen WE, Brink MF, Lagerwerf F, Worst S, van Corven E, Kostense S, Hartmann K, Weverling GJ, Uytdehaag F, Herzog C, Briggs DJ, Rupprecht CE, Grimaldi R, Goudsmit J. 2008. First administration to humans of a monoclonal antibody cocktail against rabies virus: safety, tolerability, and neutralizing activity. *Vaccine* 26:5922–5927. <https://doi.org/10.1016/j.vaccine.2008.08.050>.
  39. Lowy I, Molrine DC, Leav BA, Blair BM, Baxter R, Gerding DN, Nichol G, Thomas WD, Jr, Leney M, Sloan S, Hay CA, Ambrosino DM. 2010. Treatment with monoclonal antibodies against *Clostridium difficile* toxins. *N Engl J Med* 362:197–205. <https://doi.org/10.1056/NEJMoa0907635>.
  40. Pettitt J, Zeitlin L, Kim DH, Working C, Johnson JC, Bohorov O, Bratcher B, Hiatt E, Hume SD, Johnson AK, Morton J, Pauly MH, Whaley KJ, Ingram MF, Zovanyi A, Heinrich M, Piper A, Zelko J, Olinger GG. 2013. Therapeutic intervention of Ebola virus infection in rhesus macaques with the MB-003 monoclonal antibody cocktail. *Sci Transl Med* 5:199ra113.
  41. Skurnik D, Cywes-Bentley C, Pier GB. 2016. The exceptionally broad-based potential of active and passive vaccination targeting the conserved microbial surface polysaccharide PNAG. *Expert Rev Vaccines* 15:1041–1053. <https://doi.org/10.1586/14760584.2016.1159135>.
  42. van Duin D, Paterson DL. 2016. Multidrug-resistant bacteria in the community: trends and lessons learned. *Infect Dis Clin North Am* 30:377–390. <https://doi.org/10.1016/j.idc.2016.02.004>.
  43. Chelius MK, Triplett EW. 2000. Immunolocalization of dinitrogenase reductase produced by *Klebsiella pneumoniae* in association with *Zea mays* L. *Appl Environ Microbiol* 66:783–787. <https://doi.org/10.1128/AEM.66.2.783-787.2000>.
  44. Lees A, Nelson BL, Mond JJ. 1996. Activation of soluble polysaccharides with 1-cyano-4-dimethylaminopyridinium tetrafluoroborate for use in protein-polysaccharide conjugate vaccines and immunological reagents. *Vaccine* 14:190–198. [https://doi.org/10.1016/0264-410X\(95\)00195-7](https://doi.org/10.1016/0264-410X(95)00195-7).
  45. Varshney AK, Wang X, Cook E, Dutta K, Scharff MD, Goger MJ, Fries BC. 2011. Generation, characterization, and epitope mapping of neutralizing and protective monoclonal antibodies against staphylococcal enterotoxin B-induced lethal shock. *J Biol Chem* 286:9737–9747. <https://doi.org/10.1074/jbc.M110.212407>.
  46. Melin M, Jarva H, Siira L, Meri S, Kayhty H, Vakevainen M. 2009. *Streptococcus pneumoniae* capsular serotype 19F is more resistant to C3 deposition and less sensitive to opsonophagocytosis than serotype 6B. *Infect Immun* 77:676–684. <https://doi.org/10.1128/IAI.01186-08>.
  47. Stukes S, Casadevall A. 2014. Visualizing non-lytic exocytosis of *Cryptococcus neoformans* from macrophages using digital light microscopy. *J Vis Exp* 2014:e52084. <https://doi.org/10.3791/52084>.
  48. Fang CT, Chuang YP, Shun CT, Chang SC, Wang JT. 2004. A novel virulence gene in *Klebsiella pneumoniae* strains causing primary liver abscess and septic metastatic complications. *J Exp Med* 199:697–705. <https://doi.org/10.1084/jem.20030857>.
  49. Sheridan BS, Pham QM, Lee YT, Cauley LS, Puddington L, Lefrancois L. 2014. Oral infection drives a distinct population of intestinal resident memory CD8(+) T cells with enhanced protective function. *Immunity* 40:747–757. <https://doi.org/10.1016/j.immuni.2014.03.007>.
  50. McDonald B, Pittman K, Menezes GB, Hirota SA, Slaba I, Waterhouse CC, Beck PL, Muruve DA, Kubes P. 2010. Intravascular danger signals guide neutrophils to sites of sterile inflammation. *Science* 330:362–366. <https://doi.org/10.1126/science.1195491>.
  51. National Research Council. 2011. Guide for the care and use of laboratory animals, 8th ed. National Academies Press, Washington, DC.
  52. National Institutes of Health. 2002. Public Health Service policy on humane care and use of laboratory animals. Office of Laboratory Animal Welfare, National Institutes of Health, Bethesda, MD.